

NASA-CR-201447

Centroid detector assembly for the AXAF-I alignment test system

Paul Glenn

Bauer Associates, Inc.
888 Worcester Street, Suite 30, Wellesley, MA 02181

ABSTRACT

The High Resolution Mirror Assembly (HRMA) of the Advanced X-ray Astrophysics Facility (Imaging) (AXAF-I) consists of four nested paraboloids and four nested hyperboloids, all of meter-class size, and all of which are to be assembled and aligned in a special 15 meter tower at Eastman Kodak Company in Rochester, NY. The goals of the alignment are (1) to make the images of the four telescopes coincident; (2) to remove coma from each image individually; and (3) to control and determine the final position of the composite focus. This will be accomplished by the HRMA Alignment Test System (HATS), which is essentially a scanning Hartmann test system. The scanning laser source and the focal plane of the HATS are part of the Centroid Detector Assembly (CDA), which also includes processing electronics and software. In this paper we discuss the design and the measured performance of the CDA.

1. INTRODUCTION

The AXAF-I, which is being developed under the direction of NASA Marshall Space Flight Center with TRW as the prime contractor, comprises four nested pairs of Wolter Type I cylindrical grazing incidence mirrors. Each pair comprises first a paraboloid and then a confocal hyperboloid, both concave on their inner surfaces. Figure 1 shows a scale view of the outermost mirror pair from the AXAF-I, with approximately a 10 meter focal length and a 1.2 meter aperture diameter. It also shows, on a different scale, one-half the annular aperture. The basic reason for the difficulty in aligning cylindrical X-ray optics is that the implied required wavefront accuracies over this available annular aperture are quite small.

The following parameters describe the geometry and the alignment tolerances of the outermost AXAF-I mirror pair, with the "aperture" being defined for now at the end of the hyperbola nearer the focal plane:

$$f = \text{focal length} = 9194.8 \text{ mm} \quad (1)$$

$$r = \text{aperture radius} = 579.7 \text{ mm} \quad (2)$$

$$\Delta r = \text{annular width of the aperture} = 12.3 \text{ mm} \quad (3)$$

$$\Delta f_{\text{axial}} = \text{axial image placement error} = 0.111 \text{ mm} \quad (4)$$

$$\Delta f_{\text{lateral}} = \text{lateral image placement error} = 0.007 \text{ mm} \quad (5)$$

$$r_{\text{coma}} = \text{radius of the comatic circle} = 0.007 \text{ mm} \quad (6)$$

The parameters in Equations 1-3 describe the geometry of the system; the parameters in Equations 4-5 describe the misplacement of a perfect image; and Equation 6 describes the image degradation due to relative misalignment (lateral non-confocality) between the paraboloid and hyperboloid. (The tolerance implied by Equation 4 comes from an image radius requirement of 0.007 mm, multiplied by the ratio of f/r from Equations 1-2.) The tolerances implied by Equations 4-6 are further subdivided into measurement errors and actual residual misalignment errors.

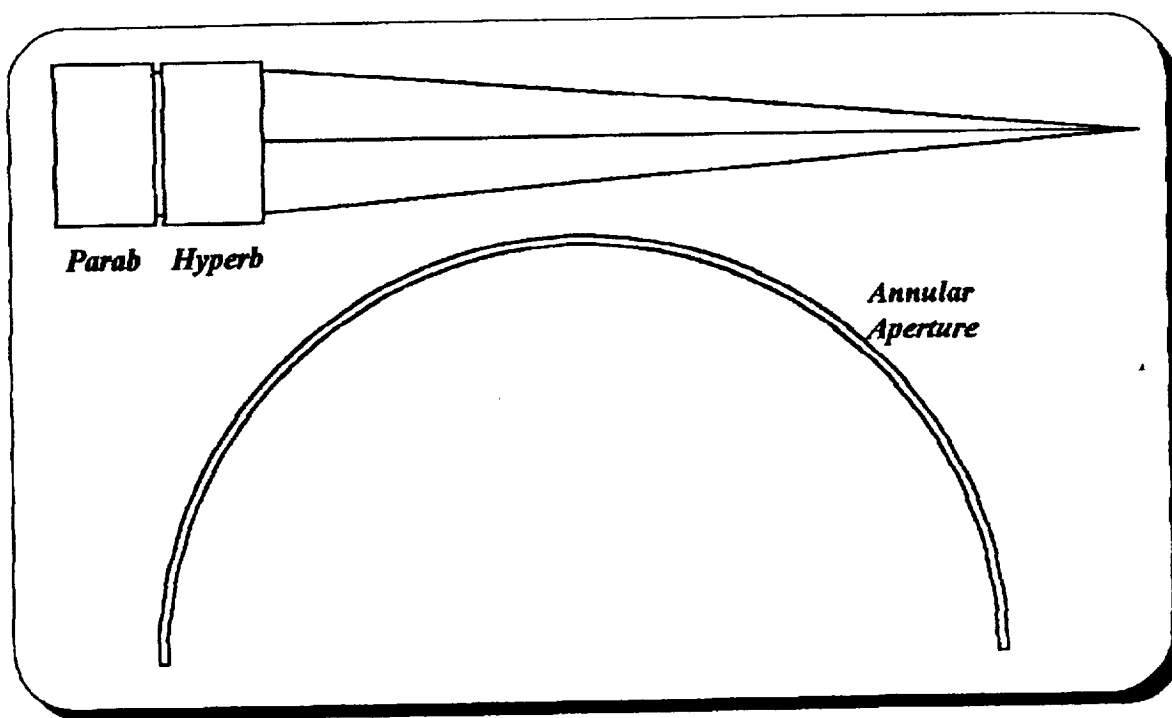


Figure 1. A scale view of the AXAF-I outermost mirror pair, and a scale view of one-half the annular aperture (different scales used). The focal length is approximately 10 meters and the aperture diameter is approximately 1.2 meters, while the annular width is only approximately 12.3 mm.

1.1. Difficulties with any interferometrically based approach

In terms of the parameters in Equations 1-6, we can use straightforward geometry to define the P-V (peak-to-valley) wavefront error implied by the various errors as follows:

$$PV_{axial} = \Delta f_{axial}(r\Delta r/f^2) = 94 \text{ Angstroms} = \lambda/67 \text{ at } 6328 \quad (7)$$

$$PV_{lateral} = \Delta f_{lateral}(2r/f) = 8827 \text{ Angstroms} = 1.39\lambda \text{ at } 6328 \quad (8)$$

$$PV_{coma} = r_{coma}(2\Delta r/f) = 187 \text{ Angstroms} = \lambda/34 \text{ at } 6328 \quad (9)$$

In short, although the lateral image placement error could be detected interferometrically, the axial image placement error and the comatic circle error would be very difficult to detect.

1.2 The modified Hartmann approach

A modified Hartmann approach was successfully used on the Technology Mirror Assembly (TMA),¹ the technology demonstration forerunner to AXAF, and in a simpler form on the High Energy Astrophysical Observatory (HEAO-B),^{2,3} this country's previous large aperture high resolution X-ray telescope. Hartmann approaches in general work by testing small sub-apertures of a system to see where in the focal plane they cast an image.⁴ Any lateral errors in the location of the image indicate a corresponding wavefront slope error at the sub-aperture being tested. By testing many sub-apertures, these slope errors can be integrated to give the total wavefront error. In a standard Hartmann approach, many sub-apertures, such as a ring of sub-apertures, are tested simultaneously, first slightly on one side of the focal plane, and then slightly on the other side.

In the modified Hartmann approach used here, a pencil beam is sent from the nominal focal point of the telescope, through the telescope, to a retro-reflection flat, back through the telescope, and back again to the nominal focal point, where its lateral location is measured. A conceptual view of this arrangement is shown in Figure 2.

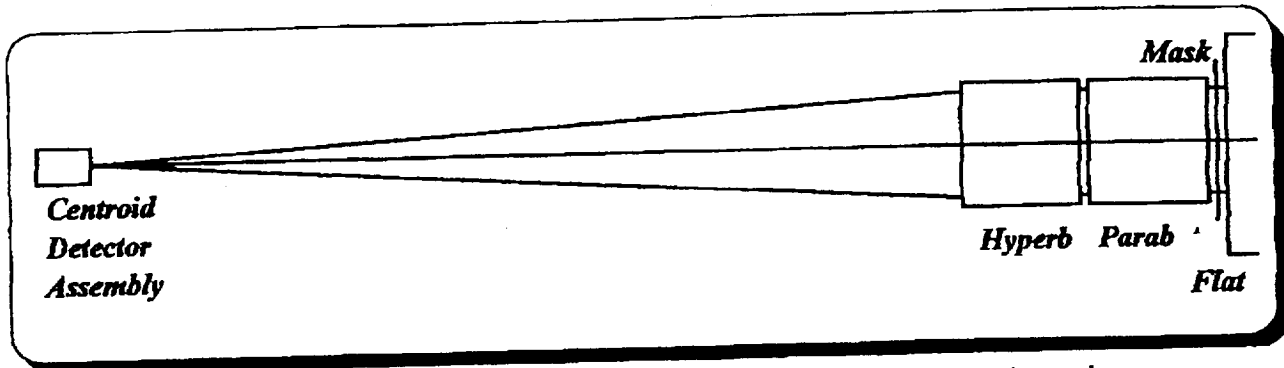


Figure 2. Conceptual layout of the Centroid Detector Assembly in use aligning a mirror pair.

2. INTERNAL CONFIGURATION

The CDA consists essentially of a laser source, beam steering optics to point the beam at various places in the annular aperture, a quadrant cell detector to sense the lateral location of the return beam, and beam splitting optics to separate the outgoing and return beams. All components are mounted in a rectangular box that is kinematically mounted to a structure in the Kodak test tower. Figure 3 shows a schematic of the internal configuration.

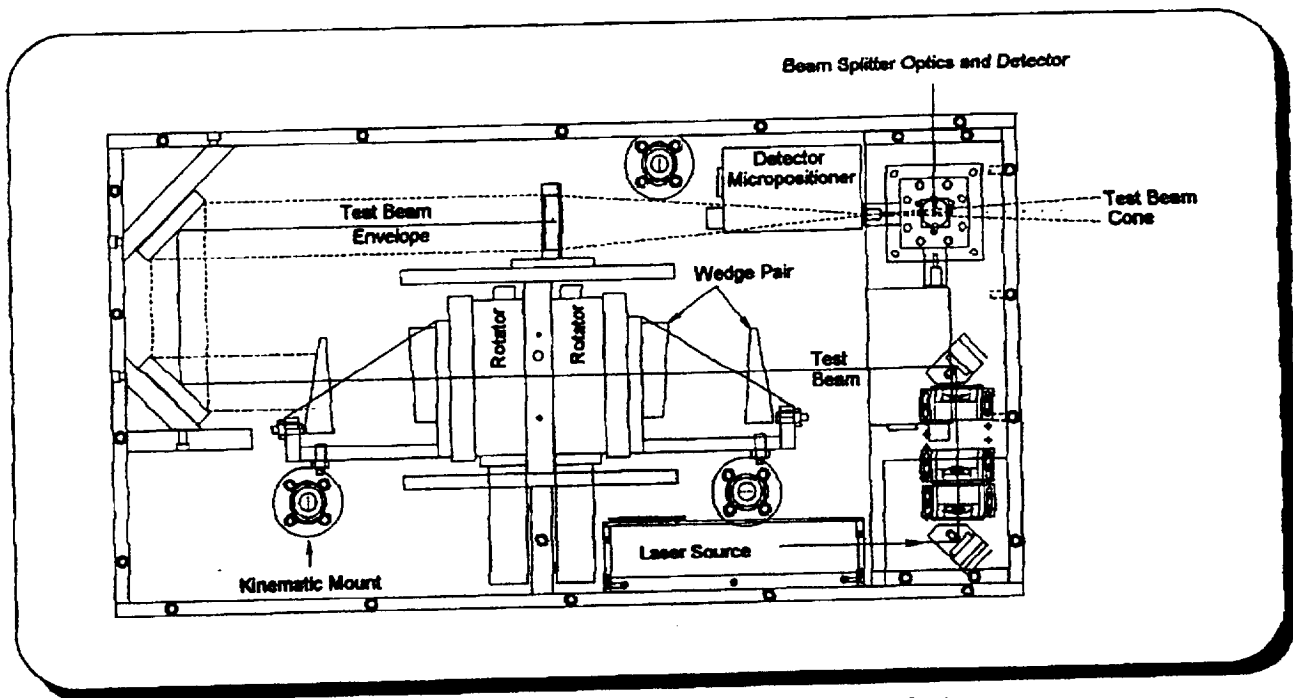


Figure 3. Schematic of the internal configuration of the CDA.

2.1. Laser source

The laser source is an innovative combination of two diode lasers, each feeding one polarization component in a single mode polarization preserving fiber. The fiber is permanently attached to the beam combining optics on one end, and to a collimating lens on the other end. (This entire assembly was specified to and supplied by Oz Optics, Ltd.) Thus, we have emanating from the collimating lens two identical and coaxial beams, each extremely clean and nearly Gaussian - one beam for a reference leg, and one for the test leg of the instrument (see Section 2.3). The beams are independently controllable (in intensity) and detectable by our electronics, so that we have complete external control over which leg of the instrument is operating.

2.2. Beam steering optics

In order to make the test beam appear to emanate from a single focal point location, but from arbitrary angles, a pair of independently tilted and rotating windows is used in the collimated space before the objective lens that focuses on the CDA's source point for outgoing test rays. Each tilted window is in fact constructed of a pair of oppositely oriented wedges, each operating at the angle of minimum deflection for stability. The opposite orientation of the wedges within a pair serves to displace the beam laterally while leaving its pointing direction unchanged. The use of two independently rotatable wedge pairs allows any composite displacement from zero to twice that of a single pair, with the composite displacement lying in any desired direction. Figure 4 shows a wedge pair, with some of the adjusters used to control the orientations of the wedges with respect to each other and with respect to the axis of the rotator. The complex detection and analytical methods used to set these orientations are beyond the scope of this paper.

2.3. Test and reference legs, and beam splitting optics

One of the important features of the CDA is the use of independent test and reference legs. The reference leg serves to monitor the position that the returned beam *would* have if it were returning from a "perfect" test piece. In this way, drifts of the laser source and the internal optics can be removed from the measurement of the position of the returned test beam. Figure 5 shows a cross section of the beam splitting optics, which are a monolithic structure specified to and procured from Meadowlark Optics. It is in these beam splitting optics that the differentiation of the test and reference beams by their polarization is important. The reference beam is reflected by the splitter, reflected by the reference sphere, and transmitted by the splitter. In contrast, the test beam is transmitted by the splitter, reflected by the optics under test, and reflected by the splitter. In either case, the beam winds up squarely on the quadrant cell where it belongs. Note that there is essentially no loss in intensity for either beam. (In Figure 5, note the use of lenses on the entrance and exit faces to minimize spherical aberration. Also note the use of a single detector for both the test and the reference beams.)

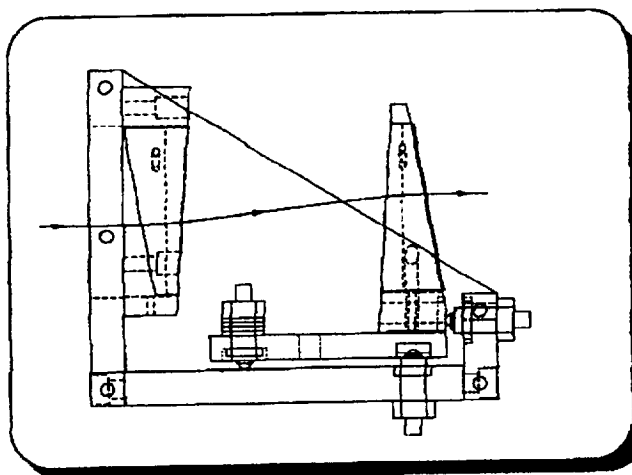


Figure 4. Wedge pair assembly. Left wedge is fixed; right wedge is adjustable with five fine adjustment screws.

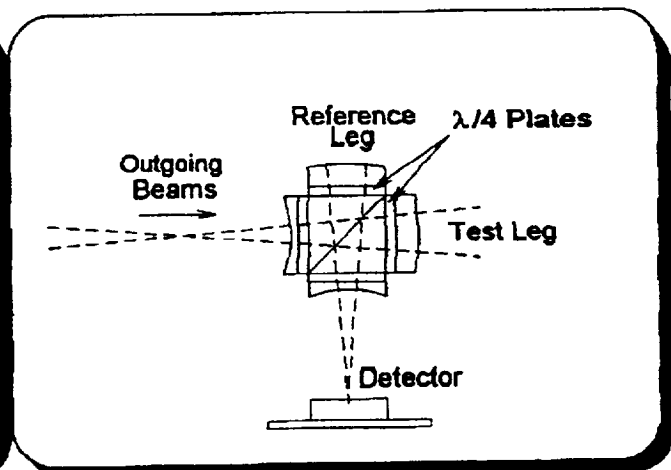


Figure 5. Beam splitting optics. Note the lenses on the entrance and exit faces to minimize spherical aberration.

2.4. Detector micropositioners, and detector calibration

Another important feature of the CDA is its ability to perform real time calibrations of the detector, using actual images. To accomplish this, the quadrant cell detector is mounted on a motorized x-y stage with 0.1 micron resolution. This allows the stage to be moved over a fine grid of known dimensions while a stationary image is present. The x- and y-positions of the stage can then be expressed as functions of the x- and y-signal values obtained from the quadrant cell. We perform a least squares fit to a polynomial series, which then defines subsequent conversions from detector values to spot positions.

3. EXTERNAL PROCESSING ELECTRONICS AND SOFTWARE

The wedge pair rotators and the detector micropositioners are controlled directly by Kodak electronics and software. In contrast, the laser control signals and the detector signals travel by cable to and from a proprietary Bauer external electronics chassis called the Centroid Detector Assembly Electronics (CDAE). The CDAE is computer-based, and has been programmed to communicate with the Kodak electronics over an unusual hybrid serial and parallel interface.

The Bauer software in the CDAE is divided into two parts. The first is our previously developed software to control and read the lasers and detectors. The second is the custom designed command interface to the Kodak electronics. We defined a set of commands that allow the Kodak electronics to accomplish the following:

- reset the CDAE
- control the intensities of the lasers
- read the test and reference signals or total power levels on the detector
- calibrate the detector

The external Kodak computer accomplishes the functions above by using a library of functions supplied by Bauer that organize the actual communications with the CDAE.

4. PERFORMANCE REQUIREMENTS

The goals of the alignment are in three separate areas:

- to make the images of the four nested telescopes coincident, both axially and laterally
- to remove coma from each of the four images individually
- to control and determine the final absolute position of the composite focus.

The first two goals depend entirely on the sensitivity, accuracy, and stability of the centroid measurement. The third goal also relies on these properties of the centroid measurement, but it also relies on careful measurement of the position of the CDA's internal focus and the orientation of the beam splitting optics. We treat each area separately below.

4.1. Control of image quality and confocality

To achieve the accurate measurement of image quality and confocality among nests, we need only discuss the sensitivity, accuracy, and stability of the centroid measurement. To do this in a rational way, it is very useful to describe, both in qualitative and in quantitative terms, the character of the centroid displacements when image quality or confocality is degraded.

The case of an image being laterally displaced is the simplest. In this case, no matter where the annular aperture is illuminated, the centroid will fall at the same place in the focal plane. In other words, as the test beam makes a full revolution about the aperture, the centroid has a constant displacement.

The case of an image being axially displaced is the next simplest. In this case, the collection of returning test beams would form a cone whose apex is at the actual focal point. When that focal point is axially displaced from the focal plane, the intersection of the cone with the focal plane is a circle. Furthermore, clearly, as the test beam makes a full revolution about the aperture, the centroid also makes a full revolution about its circle on the focal plane. And, it must be in phase with the test beam. For example, when the test beam is at an azimuth of 45 degrees on the annular aperture, the centroid must be at an azimuth of 45 degrees on its focal plane circle (or, $45 + 180 = 225$ degrees for the opposite sign of defocus).

The case of an image degraded by relative misalignment between the paraboloid and the hyperboloid is probably the most difficult to picture. However, those familiar with the coma that arises when confocal conics are misaligned will recall that at any given annular zone, the focal plane pattern is a comatic circle which is traversed twice around as the annular aperture is traversed once around. (The collection of all annular apertures gives the familiar comatic flare, which consists of all the comatic circles, each one progressively displaced further from the tip of the flare.)

The above discussion leads to the conclusion that the centroid errors can be usefully categorized according to the number of revolutions around a circle they make in the focal plane, as the test beam travels once around the annular aperture. In fact, it is a straightforward exercise in Fourier analysis to show that any centroid displacement function can be expressed as a sum of such circular functions. (This and many related analyses have been beautifully treated in detail by Kodak.³) In other words (using the (y,z) focal plane coordinate system followed in the AXAF-I alignment), if we define the (y,z) coordinates of a centroid location as the real and imaginary components of a complex number r

$$r = y + iz \quad (10)$$

then we can write the complex function r as a complex Fourier series as follows:

$$r = \sum_{m=-\infty}^{\infty} Q_m \exp(im\theta) \quad (11)$$

where each Q_m is a complex coefficient, and θ is the azimuthal angle of the test beam in the annular aperture. Also from the above discussions we can conclude that only a small number of the Q 's are relevant to alignment - specifically, Q_0 , $Re(Q_1)$, and Q_2 . (The restriction of the examination of Q_1 to its real part reflects the fact that the image circle must be traversed in phase with the aperture circle.)

And so, the CDA requirements for accuracy and stability are phrased specifically in terms of the Q -coefficients. Note that the Q -coefficients have the logical and appealing property that the magnitude of any Q -term is equal to the radius of the corresponding circle in the focal plane. Thus, the magnitude of Q_0 is the magnitude of the lateral image displacement; the magnitude of the real part of Q_1 is the radius of the focal plane circle caused by axial focus displacement; and the magnitude of Q_2 is the radius of the comatic circle.

4.2. Control and determination of the absolute position of focus

In this category there are actually two related requirements. The first is that the lateral and axial location of the apparent internal focus (i.e., the common point from which all the outgoing test rays appear to emanate) must be known to a certain tolerance.

The second (and less obvious) requirement is that when the CDA reports that the returning test beam is properly centered, then it actually *does* return to the CDA internal focus (at least within a certain tolerance). This requirement is not fulfilled unless the CDA is aligned so that the reference leg re-images the internal focus to the proper location - and, this is not a trivial condition! This requirement is referred to as achieving the proper line of sight. There was no requirement initially placed on the CDA in this area. But, through an innovative alignment technique wherein we focused the cone of outgoing test rays onto a flat for retro-reflection, we were able to achieve line of sight accuracies commensurate with our requirements on the absolute position of focus.

4.3. Summary of requirements

After a useful collaboration between Kodak and Bauer, all of the above requirements were phrased together in a cohesive fashion. Table 1 shows the results. As shown, each of the relevant Q -coefficients is broken down most broadly into static, variability during test, and variability between tests. The static error is the average error over all of the possible annular zones (four for the mirror pairs, four for the paraboloids alone, two for alignment reference mirrors, and four for optics used to set up the test tower). The variability during a test refers to the fluctuation one can expect during the course of testing all the annular

zones in succession. The variability between tests refers to the fluctuation one can expect between separate complete tests of all the annular zones.

Each of these three main areas - static, variability during a test, and variability between tests - is further subdivided into three areas - average (the average over all annular zones), zone to zone, and intrazonal. The requirements concerning absolute focus position (see Section 4.2) are contained in the average errors for Q0 and Q1. The requirements concerning image quality and confocality (see Section 4.1) are contained in all the other entries in Table 1.

	Q0	Re(Q1)	Q2
Static Errors			
Average Error	35 microns	2 microns	n/a
Zone to Zone	0.58 micron	0.58 micron	n/a
Intrazonal	n/a	n/a	0.58 micron
Variability during Test			
Average Error	n/a	n/a	n/a
Zone to Zone	0.58 micron	0.58 micron	n/a
Intrazonal	n/a	n/a	0.58 micron
Variability between Tests			
Average Error	15 microns	1.6 microns	n/a
Zone to Zone	0.58 micron	0.58 micron	n/a
Intrazonal	n/a	n/a	0.58 micron

Table 1. Requirements for measuring the various Q-coefficients, regarding both absolute position of focus, and image quality and confocality.

5. MEASURED PERFORMANCE

In this section we review the performance measured before delivery to Kodak. (Note that the performance after delivery is an entirely different topic⁶ - not because the instrument's inherent performance changed, but because the testing environment was completely different.) Table 2 gives the achieved accuracies in exactly the same format as Table 1.

There are two values in Table 2 (static zone to zone errors for Q0 and Q1), shown in bold type with asterisks, that are slightly higher than the original requirements. The requirements were relaxed accordingly before delivery. Note that all the other accuracies exceed the requirements, often by a healthy margin.

To get an intuitive idea of the accuracy of these alignment measurements, one can note that the plate scale is approximately 100 microns in the focal plane per arc-second of error in the single-pass configuration. (This is twice the nominal plate scale of 50 microns per arc-second, because the CDA is testing the optics in a double pass configuration.) Therefore, the tightest accuracy requirement taken from Table 1 of 0.58 micron boils down to 0.006 arc-second. In short, the CDA is capable of measuring image degradation due to misalignment of the 1.2 meter AXAF-I telescope on the order of 0.006 arc-second. This is only on the order of two percent of the total projected on-orbit image degradation.

Finally, Figure 6 gives a visual demonstration of the accuracy and stability of the CDA by showing the progression of the measurement of the relevant Q-coefficients over a 15 hour period.

	Q0	Re(Q1)	Q2
Static Errors			
Average Error	6.71 microns	0.51 micron	n/a
Zone to Zone	0.74 micron**	0.79 micron**	n/a
Intrazonal	n/a	n/a	0.52 micron
Variability during Test			
Average Error	n/a	n/a	n/a
Zone to Zone	0.47 micron	0.27 micron	n/a
Intrazonal	n/a	n/a	0.29 micron
Variability between Tests			
Average Error	2.2 microns	0.27 micron	n/a
Zone to Zone	0.47 micron	0.27 micron	n/a
Intrazonal	n/a	n/a	0.24 micron

Table 2. Achieved accuracies, for comparison with Table 1.

Drift of Q-coefficients through 15 hours

Zone = MP1 (semi-cone angle = 3.458 degrees)

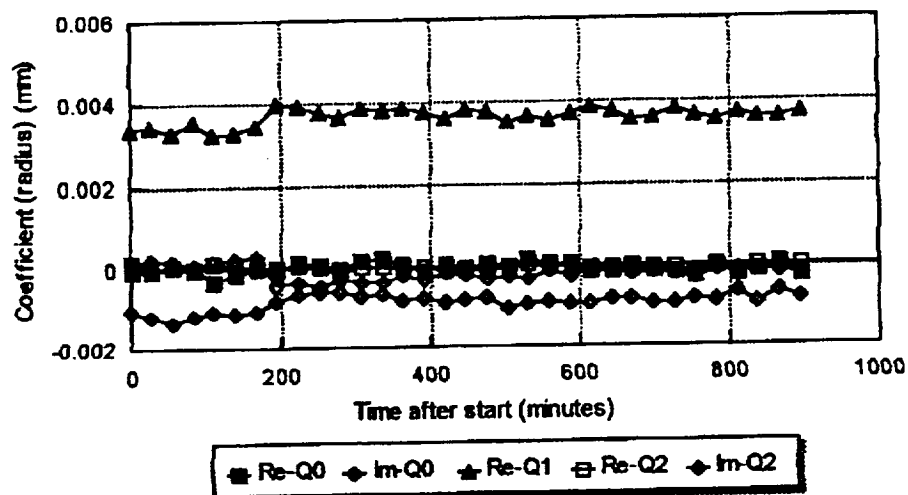


Figure 6. Drift in the measurement of the relevant Q-coefficients over 15 hours.

As shown in Figure 6, all of the fluctuations are easily in the sub-micron range. Moreover, even the absolute values are in the sub-micron range (except for Q1, whose four micron bias simply indicated that the CDA was not quite in focus during the test).

6. ACKNOWLEDGMENTS

This work was performed under contract to Eastman Kodak Company, which is under contract to TRW, which is in turn the prime contractor to NASA Marshall Space Flight Center. The AXAF-I cylindrical optics were manufactured by Hughes Danbury Optical Systems. The author wishes to thank those at Bauer (particularly John Glenn) and Kodak (particularly Mark Waldman) who contributed long hours and good ideas that helped the instrument achieve its excellent performance.

7. REFERENCES

1. N. DeFilippis, P. Glenn, and R. Cahill, "Assembly and alignment of the AXAF/TMA," *Proc. SPIE* 640, 155 (1986).
2. L. P. VanSpeybroeck, "Design fabrication and expected performance of the HEAO-B X-ray telescope," *Proc. SPIE* 106, 136 (1977).
3. L. P. VanSpeybroeck, "Einstein observatory (HEAO-B) mirror design and performance," *Proc. SPIE* 184, 2 (1979).
4. D. Malacara, *Optical Shop Testing*, John Wiley and Sons, New York, 1978.
5. T. Lewis, "AXAF-I alignment test system autocollimating flat error correction," *Proc. SPIE* 2515 (1995).
6. M. Waldman, "The alignment test system for AXAF-I's High Resolution Mirror Assembly," *Proc. SPIE* 2515 (1995).